Since January 2020 Elsevier has created a COVID-19 resource centre with free information in English and Mandarin on the novel coronavirus COVID-19. The COVID-19 resource centre is hosted on Elsevier Connect, the company's public news and information website.

International Journal of Biochemistry and Cell Biology 152 (2022) 106299

Contents lists available at ScienceDirect

International Journal of Biochemistry and Cell Biology

journal homepage: www.elsevier.com/locate/biocel

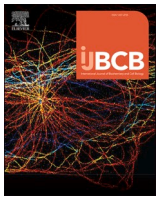

B-cell receptor associated protein 31 deficiency decreases the expression of adhesion molecule CD11b/CD18 and PSGL-1 in neutrophils to ameliorate acute lung injury

Guo-xun Li [a], Xiao-han Jiang [a], Jing-nan Zang [a], Ben-zhi Zhu [a], Cong-cong Jia [b], Kun-wei Niu [c], Xia Liu [a], Rui Jiang [a,*], Bing Wang [a,*]

[a] Institute of Biochemistry and Molecular Biology, College of Life and Health Sciences, Northeastern University, Shenyang 110819, China
[b] Liaoning Provincial Key Laboratory for Research on the Pathogenic Mechanisms of Neurological Diseases, The First Affiliated Hospital, Dalian Medical University, Dalian 116011, China
[c] Department of Hepatobiliary Surgery, Xijing Hospital, Fourth Military Medical University, 127 Changle Road, Xi'an, Shaanxi 710032, China

ARTICLE INFO

Keywords:
BAP31
Acute lung injury
Neutrophil adhesion
CD11b/CD18
PSGL-1

ABSTRACT

Acute lung injury (ALI) and its more severe condition acute respiratory distress syndrome (ARDS) are critical life-threatening disorders characterized by an excessive influx of neutrophils into the alveolar space. Neutrophil infiltration is a multi-step process involving the sequential engagement of adhesion molecules. The adhesion molecule CD11b/CD18 acts as an important role in the recruitment of neutrophils to lung tissues in the ALI model. B-cell receptor associated protein 31 (BAP31), an endoplasmic reticulum transmembrane protein, has been reported to regulate the cellular anterograde transport of CD11b/CD18 in human neutrophils. To explore how BAP31 regulates CD11b/CD18 in mouse neutrophils, we constructed myeloid-specific BAP31 knockdown mice in this study. Biological investigations indicated that BAP31 deficiency could significantly alleviated lung injury, as evidenced by the improved histopathological morphology, reduced pulmonary wet/dry weight ratio, inhibited myeloperoxidase level and decreased neutrophil counts in the bronchoalveolar lavage fluid. Further studies clarified that BAP31 deficiency obviously down-regulated the expression of CD11b/CD18 and P-selectin glycoprotein ligand-1 (PSGL-1) by deactivating the nuclear factor kappa B (NF-κB) signaling pathway. Collectively, our results revealed that BAP31 depletion exerted a protective effect on ALI, which was possibly dependent on the attenuation of neutrophil adhesion and infiltration by blocking the expression of adhesion molecules CD11b/CD18 and PSGL-1. These findings implied the potential of BAP31 as an appealing protein to mediate the occurrence of ALI.

1. Introduction

Acute lung injury (ALI) and its more serious form, acute respiratory distress syndrome (ARDS), have constituted a major threat to human health with high morbidity and mortality rates. The clinical manifestations are predominately characterized by hypoxemic respiratory failure and bilateral pulmonary infiltration (Butt et al., 2016; Ware, 2006). During the pathogenetic progression of ALI, polymorphonuclear neutrophils (PMNs) recruitment from blood vessels to tissues is a critical prerequisite (Fine et al., 2019; Maas et al., 2018). The classical cascade of neutrophil recruitment is a precision-regulated dynamic process, commonly divided into following procedures: capture, rolling, arrest, adhesion, crawling, and transendothelial migration (Muller, 2013; Silvestre-Roig et al., 2020). In particular, the adhesion of PMNs to endothelial cells (ECs) mediated by cell adhesion molecules (CAMs) is well-recognized as an important link in the multiple-step cascade (Dianzani et al., 2003; Wang and Doerschuk, 2002). Although some great strides have been made towards acknowledging the pathogenesis of ALI in the past decades, the therapeutic outcome has still not been markedly improved (Standiford and Ward, 2016). Accordingly, searching for novel strategies for the prevention and treatment of ALI is extremely urgent.

B-cell receptor associated protein 31 (BAP31 or BCAP31) has been identified as an evolutionarily conserved, and ubiquitously expressed

* Corresponding authors.
E-mail addresses: jiangrui@mail.neu.edu.cn (R. Jiang), wangbing@mail.neu.edu.cn (B. Wang).

https://doi.org/10.1016/j.biocel.2022.106299
Received 24 May 2022; Received in revised form 31 August 2022; Accepted 18 September 2022
Available online 19 September 2022

polytopic integral protein in the endoplasmic reticulum (ER) (Annaert et al., 1997). The gene is localized at Xq28 (Adachi et al., 1996). Early findings have reported that the C-terminal domain of BAP31 is selectively cleaved into a proapoptotic fragment (P20) by caspase-8, which directly mediates apoptosis progression (Iwasawa et al., 2011; Ng et al., 1997; Wang et al., 2011). BAP31 is highly expressed in neurons and involved in regulating neuronal apoptosis. Mutation of BAP31 can cause a critical severe X-linked phenotype such as motor and intellectual disabilities or sensorineural deafness (Cacciagli et al., 2013). Our previous studies have found that BAP31 performs a significant role in T cell activation, the ER-associated protein degradation (ERAD) pathway, insulin resistance, hepatic lipid accumulation, and gastric cancer proliferation (Chen et al., 2019; Jia et al., 2018; Niu et al., 2017; Wang et al., 2008; Xu et al., 2018). Functionally, BAP31 acts as a sorting factor that participates in the transportation of various protein molecules from ER to Golgi apparatus, *e.g.* class I major histocompatibility complex (MHC-I), protein tyrosine phosphatases like B and membrane-associated RING-CH (MARCH) (Bartee et al., 2010; Ladasky et al., 2006; Wang et al., 2004).

In addition to these canonical functions, prior publications have confirmed that BAP31 can bind to CD11b/CD18 ($\alpha_M\beta_2$ Mac-1, CR3) in the secondary granules of human neutrophils, thus mediating their trafficking to cell membrane surface (Zen et al., 2004). As a member of β2-integrin, the structural characteristics and distribution of CD11b/CD18 lay a foundation for their participation in neutrophil recruitment, exudation, migration and inflammatory response (Friedrichs et al., 2014; Tan, 2012; Wee et al., 2015). In resting state, CD11b/CD18 is mainly present in the secondary granules of neutrophils. Upon cells activation, the translocation of CD11b/CD18 from intracellular pools to the plasma membrane ensures PMNs-ECs adhesion by combining with intercellular adhesion molecule 1 (ICAM-1), thereby leading to an influx of PMNs into tissues and initiating inflammatory response (Berger et al., 1984; Jerke et al., 2013; Johnson-Léger and Imhof, 2003; Zen et al., 2004). In the ALI model, the combination of CD11b/CD18 with surface receptor ICAM-1 on alveolar vascular ECs results in the accumulation of PMNs into lung tissue and aggravation of pulmonary inflammation (Hou et al., 2014; Issekutz et al., 1999). Furthermore, the selectin family is primarily responsible for regulating the primary adhesion of neutrophils and intracellular signal transduction (Crockett-Torabi, 1998). As a co-ligand of the selectin family, P-selectin glycoprotein ligand-1 (PSGL-1) is constitutively expressed at the tip of neutrophil microvilli, the unique spatial location of which decides it the earliest to participate in PMNs-ECs interactions (Hidari et al., 1997; Yang et al., 1999).

Inspired by the foregoing studies, we attempted to establish myelocyte-specific BAP31 knockout mice using the Cre/loxP recombination system to explore which adhesion molecules are regulated by BAP31. In this study, we observed that neutrophil infiltration into lung tissues under inflammation was substantially reduced with the loss of BAP31, which was caused by a marked decline in the adhesion level of neutrophils to ECs. These results demonstrated that BAP31 may participate in the functional regulation of various inflammation-associated adhesion molecules. For this reason, adhesion molecules affected by BAP31 deficiency in neutrophils were systematically screened. The molecular mechanism of their effect on PMNs-ECs adhesion was also investigated. The result showed that BAP31 knockdown could evidently down-regulated the transcriptional level of CD11b/CD18 and PSGL-1, which may be associated with the nuclear factor kappa B (NF-κB) signaling pathway. Interestingly, the immunoprecipitation assay found that BAP31 could bind to CD11b/CD18, but not to PSGL-1 in mice, which was consistent with previous observations on human neutrophils. These results highlighted the significant modulation of BAP31 on adhesion function of CD11b/CD18 by distinct mechanisms. Our findings implicated BAP31 as a crucial molecule for affecting the occurrence of ALI.

2. Material and methods

2.1. Animals

To obtain mice that specifically lacked BAP31 in neutrophils, we inserted the loxP site on both sides of exon 3 of BAP31 gene to construct a targeting vector. The targeting vector also carried a neomycin resistance gene, which was located in the loxP site with two FRT sites on both sides. The neomycin resistance gene is an exogenous marker gene for resistance screening of transgenic mouse embryonic cells. Targeted vectors were transferred to mouse embryonic stem (ES) cells by electroporation, and stem cells were obtained from C57BL/6 mice. Homologous recombinants were screened with G418 and then analyzed by Southern blotting and PCR. The constructed female mice were used to delete neomycin in *vivo* by breeding with male FLPeR mice (Farley et al., 2000). Lyz2-Cre enzymes are expressed only in myeloid cells, but not in other tissues. The Cre enzyme was reorganized to remove the BAP31 gene sequence from myeloid cells. Under the control of Lyz2 promoter enhancer, mice expressing Cre recombinase were cultured as mice with defective BAP31 in myeloid cells. $BAP31^{flox/+}$ mice were bred with Lyz2-Cre mice to produce $BAP31^{flox/flox}$ Lyz2-Cre ($BAP31^{-/-}$) mice and littermate controls $BAP31^{flox/flox}$ ($BAP31^{+/+}$) mice. Next, we used the above two types of sex and age matched littermates. The genotypes of these mice were determined by PCR gene identification ($BAP31^{f/f}$ primers: sense 5′-AAGGGGAGCCAGGAATAGTGGTG-3′; antisense 5′-TCCTGGCAGTTTCCAGTAAGGGTAAC-3′; Cre primers: sense 5′-CCCAGAAATGCCAGATTACG-3′; antisense 5′-CTTGGGCTGCCAGA ATTTCTC-3′).

Blood samples were collected into tubes containing ethylene diamine tetraacetic acid K2 (EDTA-K2) to measure the numbers of leukocytes and neutrophils using automated hematology analyzers at the Animal Hospital of Shenyang Agricultural University. The process from sampling to analysis was performed according to the procedures in the hospital' clinical laboratories. All mice were maintained at room temperature without pathogen and 12 h of light/dark circulation. Mice feed, litter and drinking water bottles were autoclaved, and the animals were free to eat and drink water. Body weight was measured once a week using a digital electronic balance. All experimental procedures were critiqued and approved by the Committee of Experimental Animal Administration of Northeastern University in accordance with the National Institutes of Health' Guidelines for the Care and Use of Laboratory Animals.

2.2. Histopathological evaluation

LPS (5 mg/kg) was injected into 6–8 weeks old C57BL/6 mice after 24 h injection by tail vein to induce lung injury. After harvesting the lungs of different treated mice, they were placed into 4% paraformaldehyde (PFA) fixing solution for overnight, dehydrated using graded ethanol and xylene, embedded with paraffin and sliced into 5 μm sections. After dewaxing and hydration, the slices were immersed in hematoxylin and eosin (H&E) reagent following a standard protocol, and pathological alterations were visualized under a light microscope.

According to alveolar congestion, hemorrhage, inflammatory cell infiltration and edema, lung injury was evaluated using a semi-quantitative scoring system (0: normal; 1: mild or small amounts; 2: moderate or more amounts; 3: severe or large amount; 4: extremely severe or extremely large amount). All scores were calculated for the statistical analysis.

After LPS exposure at 24 h, lung tissues were removed. The surface water was absorbed with a filter paper. The wet weight was measured and recorded. Subsequently, the lungs were incubated in an oven at 80 °C for 48 h to determine dry weight. The wet-to-dry weight ratio was calculated.

2.3. Measurement of leukocyte influx and protein content in bronchoalveolar lavage fluid (BALF)

After the lungs were lavaged with 1 mL PBS for three times, BALF was collected as described previously (Mutlu et al., 2007). The collected BALF samples were used to detect the number of total cells under a standard hemocytometer. The remaining BALF was centrifuged immediately at 1000g at 4 °C for 10 min to obtain the supernatant and cell pellets. The supernatant was used to determine the total protein concentrations by a BCA protein assay kit (Beyotime). In addition, the sedimented cells were resuspended in PBS and smeared onto slides. Wright-Giemsa staining of the prepared smears was performed to count the number of neutrophils using a light microscope according to the morphological criteria of neutrophils.

2.4. Measurement of MPO level

After LPS administration for 24 h, the myeloperoxidase (MPO) activity was evaluated using commercially available kits according to the manufacturer's instructions (Nanjing jiancheng Technology Co., Ltd, Nanjing, China). The right lung was made into a 5% tissue homogenate, which was treated with MPO activity detection reagent for 15 min at 37 °C. The developer mix was added to the control and measurement tubes, and incubated at 37 °C for 30 min. Then, the MPO color reagent was added to the above samples for 10 min in 60 °C water bath. After removal of the tube from water bath, the absorbance values of each tube were immediately measured at 460 nm.

2.5. Immunofluorescence analysis

The collected lung tissues were fixed with 4% paraformaldehyde solution for 24 h, dehydrated using graded ethanol and xylene, embedded in paraffin and sectioned into 5 μm slices. Following deparaffinization, hydration and epitope retrieval, slides were washed with PBS and blocked with goat serum. The thicknesses were incubated with primary antibody (abs125388a; Absin Bioscience, Inc., Shanghai, China) against MPO (1: 200) at 4 °C overnight in a humidity box, followed by fluorescence-labeled secondary antibodies (abs20023; Absin Bioscience, Inc., Shanghai, China) at room temperature for 1 h. Nuclei were counter-stained with Hoechst 33342. All the sections were examined and photographed using a fluorescence microscope. The average number of cells/field of view was used for the statistical analysis.

2.6. Intravital microscopy

6–8 weeks old C57BL/6 mice were injected with LPS (20 mg/kg) by the tail vein. The control group was injected with the same volume of saline, and the model was successful after 4 h. After 4 h, the mice were injected with 50 μL of rhodamine 6 G (1 mg/mL, Sigma) to fluorescently label the leukocytes. Leukocytes adhering to the vascular endothelium were observed under an intravital microscope. Leukocytes at 30 s without significant movement were defined as adhesions.

2.7. Neutrophils purification and in vitro adhesive assay

Following the manufacturer's instructions (Beijing Solarbio Science & Technology Co., Ltd), neutrophils were isolated and purified from mouse bone marrow. Purified neutrophils were treated with LPS and labeled with Hoechst 33342. Prior to the assay, b.End3 cells were plated onto 24-well culture plates at a density of 5×10^4 cells/well for 24 h. The labeled PMNs (2×10^5 cells/well) were incubated with pre-prepared b.End3 cells at 37 ℃ for 30 min. After washing non-adherent neutrophils with PBS three times, the adherent cells were measured using a fluorescence microscope (Leica, Wetzlar, HE, Germany).

2.8. Flow cytometric assay

Purified neutrophils were exposed to LPS, washed with PBS and resuspended in 100 μL of 5% BSA solution in an EP tube. After incubation on ice for 10 min, the primary antibodies CD11b (101212; BioLegend), CD18 (101414; BioLegend), and PSGL-1 (555306; BD Biosciences) were used to stain the target proteins for 45 min in ice water bath. Later, the cells were centrifuged (1000 rpm, 5 min) and washed twice with PBS. The collected cells were resuspended in 300 μL PBS and immediately analyzed using a flow cytometer (Becton Dickinson, NJ, USA).

2.9. Real-time PCR assay

Total RNA of neutrophils was extracted with TRIzol reagents (Carlsbad, CA, USA). Two-microgram total RNA was used for reverse transcription into cDNA (Promega, Madison, USA). Quantitative real-time PCR (RT-qPCR) was implemented by Go Taq® qPCR Master (Promega, Madison, USA). The expression level of each mRNA relative to GAPDH expression was analyzed via the ΔΔCt method. The PCR primers for BAP31, PSGL-1, ESL-1, CD11b, CD29, CD11a, CD18, CD11c, CD44, L-selectin, VLA-1, CD49d and GAPDH are listed in Supplementary Table S1.

2.10. Western blot analysis

Treated cells were harvested and lysed with radioimmunoprecipitation assay (RIPA) lysis buffer containing 1% protease inhibitor cocktail, 1% phosphatase inhibitor cocktail, and 1 mM phenylmethanesulfonyl fluoride (PMSF). Protein concentration was measured using a bicinchoninic acid (BCA) protein assay kit (Beyotime Biotechnology Co., Shanghai, China). Equal amounts of protein were separated by 8%–12% sodium dodecyl sulfate polyacrylamide gel electrophoresis (SDS-PAGE), electroblotted onto polyvinylidene difluoride (PVDF) membranes (Millipore, Billerica, MA), and blocked with 5% skimmed milk for 60 min at room temperature (rt). Membranes were incubated with specific primary antibodies overnight at 4 °C. After washing three times with TBST (5 min ×3), the membranes were probed with the corresponding secondary antibodies for 1–2 h at rt. Then, protein bands were detected with ECL Select Western blot detection reagent (Millipore, Billerica, MA, USA) by chemiluminescence (Tanon 5500, Shanghai, China). Each protein band was calculated and normalized to that of β-actin/Histone H3. Image Lab software (Tanon, Shanghai, China) was used for quantitative grayscale analysis of the bands. The details of antibodies were shown as follows: anti-Histone H3 (abs130594a; Absin Bioscience), anti-NF-κB p65 (8242; Cell Signaling Technology), anti-p-IKKα/β (2697; Cell Signaling Technology), anti-p-IκBα (2859; Cell Signaling Technology), anti-IκBα (4814; Cell Signaling Technology), anti-CD11b (AF6396; Beyotime), anti-CD18 (AF6399; Beyotime), anti-PSGL-1 (NB100–78039; NOVUS), anti-BAP31 (11200–1-AP; Proteintech Group Inc.) and anti-β-actin (66009–1-Ig; Proteintech Group Inc.).

2.11. Immunoprecipitation (IP) assay

Neutrophils were lysed with NP40 buffer for 30 min in an ice bath. The lysates were centrifuged to collect the supernatants, which were mixed with protein G agarose beads (Invitrogen) for 1 h. After centrifugation, the supernatants were incubated with pull-down antibodies for 2 h. After the addition of G Sepharose beads, the complexes were centrifugated, washed three times, resuspended in SDS loading buffer and boiled for 10 min. The supernatants were loaded onto SDS-PAGE gel. Electrophoresis was performed and analyzed using Western blotting, as described above.

2.12. Statistical analysis

All experimental data are presented as mean±SEM of at least three independent data points. The statistically significant differences between groups were assessed using unpaired Student's *t*-test or one-way ANOVA. Analyses were performed using ImageJ software and GraphPad Prism 5.0. * ** $p < 0.001$, * * $p < 0.01$ or * $p < 0.05$ was considered statistically significant.

3. Results

3.1. Generation and identification of myeloid-specific BAP31 deletion mice

The simultaneous deletion of a gene in an organism can produce undesirable consequences, such as biological dysfunction (Zhang et al., 2012). To this end, we constructed BAP31 conditional knockout mice specifically in myeloid cells using Cre-loxP tissue-specific gene targeting. The system consists of two components: mice have two loxP sites located on two flanks of exon 3 of the BAP31 gene; mice carry Lyz2-Cre recombinase. Lyz2-Cre, an enzyme specifically expressed in myeloid cells catalyzes the recombination of two loxP sites and resects the fragment between two loxP sites, resulting in the retention of one loxP site (Supplementary Fig. S1A). As shown in Supplementary Fig. S1B, the types of mice were identified by analyzing their DNA genomes. Real-time PCR analysis of mRNA from myeloid cells demonstrated that the mRNA level of BAP31 was significantly declined in BAP31$^{-/-}$ mice compared with BAP31$^{+/+}$ mice (Fig. 1A). Again, an obvious reduction in BAP31 protein expression was observed (BAP31$^{-/-}$ mice versus BAP31$^{+/+}$ mice, Fig. 1B, C). To assess whether the loss of BAP31 impacted the normal growth and development of mice, we measured the body weight of mice every other week for eight weeks. There were no significant differences in body weight between the two groups, suggesting that myeloid cells BAP31 disruption did not affect the growth conditions of mice (Fig. 1D). Additionally, the number of leukocytes and neutrophils in the peripheral blood fluctuated within the reference range and did not reach statistical distinctions between 8-wk-old and 24-wk-old mice (Fig. 1E, F). These results revealed that the myeloid cells-specific BAP31$^{-/-}$ mouse model was successfully established, and the growth of mice was not influenced.

To investigate the influence of myeloid-specific BAP31 knockdown on the growth and development of lung tissues, we examined the morphological and histological characteristics of lung tissues. The surface of lung tissues in both BAP31$^{+/+}$ and BAP31$^{-/-}$ groups was smooth, and had no obvious hyperemia and swelling, indicating that BAP31 deficiency did not cause morphological variation of lung tissues (Supplementary Fig. S2A). Furthermore, the lung weight coefficient, an indicator of pulmonary edema, had no statistical significance between BAP31$^{+/+}$ and BAP31$^{-/-}$ groups (Supplementary Fig. S2B). Consistently, the hematoxylin and eosin (H&E) staining showed a normal alveolar morphology without lung edema, diffuse hemorrhage, alveolar collapse and alveolar septal thickening in both BAP31$^{+/+}$ and BAP31$^{-/-}$ groups (Supplementary Fig. S2C). Therefore, these observations revealed that myeloid-specific BAP31 knockdown did not affect normal growth and development of lung.

3.2. Effects of BAP31 knockdown on body weight, histopathological variations and pulmonary edema in LPS-induced ALI mice

Using an in *vivo* LPS-induced ALI mouse model, we initially inspected the influences of BAP31 on body weight. With regard to the BAP31$^{+/+}$ and BAP31$^{-/-}$ groups, there was no significant difference in body weight after saline treatment (Supplementary Fig. S3). Compared with saline+BAP31$^{+/+}$ group, the body weight was dramatically reduced in LPS+BAP31$^{+/+}$ group, suggesting that the body weight of mice was reduced by LPS stimulation. Nevertheless, the loss of body weight in LPS+BAP31$^{-/-}$ group exhibited an obvious decrease by comparison with LPS+BAP31$^{+/+}$ group. These results indicated that BAP31 deficiency possessed a certain protective effect on the body weight of mice following LPS challenge.

Afterwards, the effects of BAP31 deficiency on the morphological and histopathological features of lung tissues were also detected. As depicted in Fig. 2A, the surface of pulmonary tissue appeared pink, smooth, and had no visible leakage or bleeding in the saline-injected groups. After LPS stimulation, the gross appearance of lung tissue showed dark red hemorrhages and severe damage, which were largely alleviated by the depletion of BAP31. In addition, H&E staining showed that LPS exposure resulted in an obvious disorder of lung tissue structure along with a severe pathomorphology such as lung edema, PMN infiltration, diffuse hemorrhage, alveolar collapse and alveolar septal thickening. By contrast, BAP31 knockdown could attenuate LPS-stimulated histologic damage (Fig. 2B). Consistent with the above analyses, the score of LPS-treated BAP31$^{-/-}$ mice was dramatically reduced as compared to that of LPS-treated BAP31$^{+/+}$ mice (Fig. 2C). Subsequently, the severity of pulmonary edema in lungs was measured using the W/D ratio. After 24 h of LPS challenge, the lung W/D ratio in BAP31$^{+/+}$ group was apparently higher than that in BAP31$^{-/-}$ group (Fig. 2D). These results indicated that BAP31 deficiency could alleviate

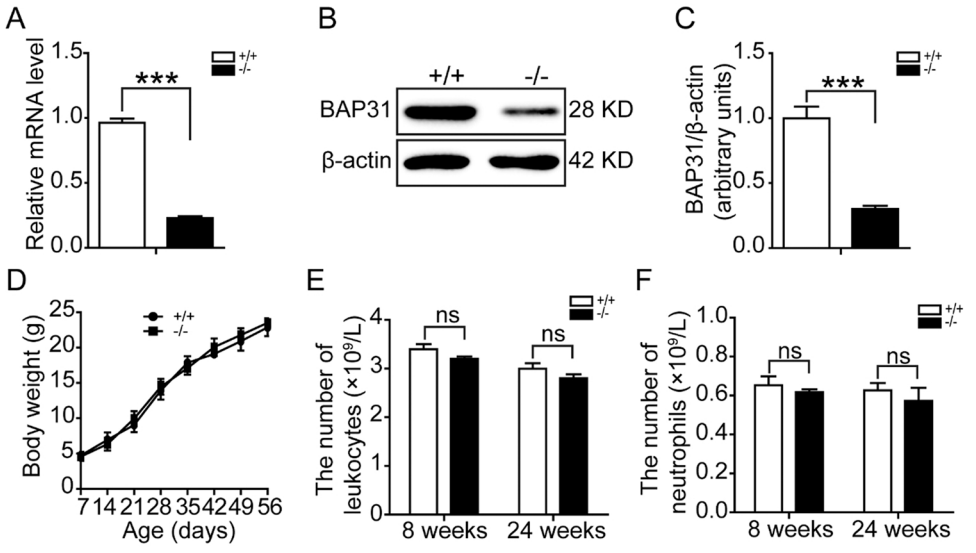

Fig. 1. Characterization of myeloid-specific BAP31 deletion mice. (A) mRNA expression of BAP31 from BAP31$^{-/-}$ and BAP31$^{+/+}$ mice analyzed by Real-time PCR (BAP31$^{+/+}$, n = 3; BAP31$^{-/-}$, n = 3). (B, C) Protein expression of BAP31 detected by Western blotting (BAP31$^{+/+}$, n = 3; BAP31$^{-/-}$, n = 3). (D) Variation of mice body weight was measured (BAP31$^{+/+}$, n = 6; BAP31$^{-/-}$, n = 6). (E, F) The amounts of leukocytes and neutrophils were monitored (BAP31$^{+/+}$, n = 3; BAP31$^{-/-}$, n = 3). The values were shown as mean ± SEM, *** $p < 0.001$. ns, not significant.

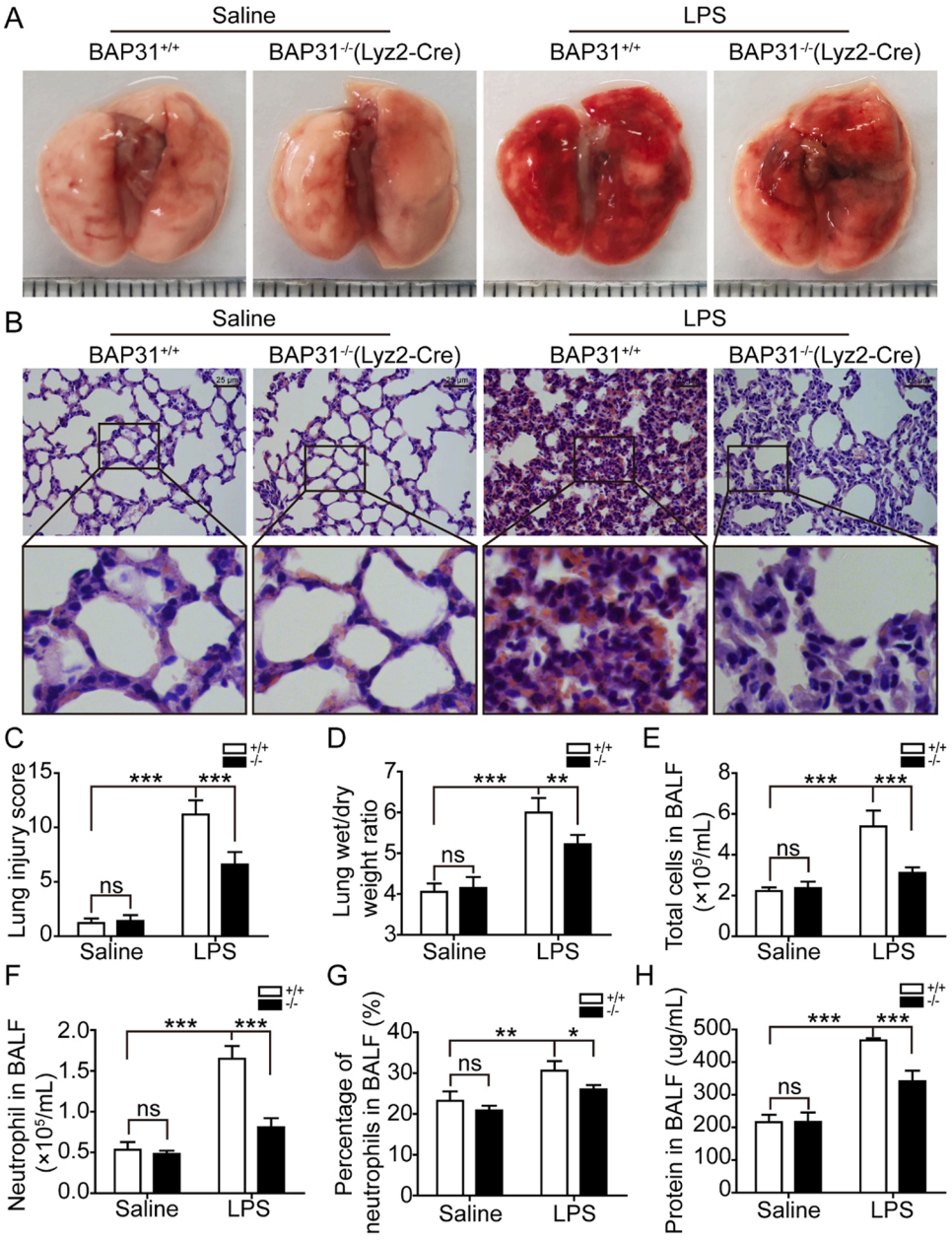

Fig. 2. Effects of BAP31 knockdown on histopathological changes and pulmonary edema in LPS-induced ALI mice. (A) Representative photographs of lung tissues from different groups. (B) Representative histological changes of lung obtained from mice of different groups (Scale bars: 25 μm). (C) Lung injury score counted by semi-quantitative analysis (Saline+BAP31$^{+/+}$, n = 5; Saline+BAP31$^{-/-}$, n = 5; LPS+BAP31$^{+/+}$, n = 5; LPS+BAP31$^{-/-}$, n = 5). (D) Lung water content calculated as a ratio of wet weight to dry weight (Saline+BAP31$^{+/+}$, n = 4; Saline+BAP31$^{-/-}$, n = 4; LPS+BAP31$^{+/+}$, n = 4; LPS+BAP31$^{-/-}$, n = 4). (E) Total cell number, (F) neutrophils, (G) Percentage of neutrophils and (H) protein concentration in BALF (Saline+BAP31$^{+/+}$, n = 3; Saline+BAP31$^{-/-}$, n = 3; LPS+BAP31$^{+/+}$, n = 3; LPS+BAP31$^{-/-}$, n = 3). The values were shown as mean ± SEM, * $p < 0.05$, ** $p < 0.01$, *** $p < 0.001$. ns, not significant.

the pulmonary pathological morphology in ALI.

After exposure to LPS, the major parameters, containing total cells, neutrophils and protein content in BALF, were measured. Total cells number, neutrophil counts and the percentage of neutrophils were obviously increased in the LPS-challenged groups compared to those in saline groups. However, the number and proportion of neutrophils in LPS-stimulated BAP31$^{-/-}$ group were substantially lower than those in LPS-alone group, signifying that the deletion of BAP31 could reduce excessive PMNs infiltration during ALI (Fig. 2E-G). Likewise, LPS exposure in mice displayed a serious lung edema, as evidenced by an elevated protein content in BALF (versus saline-treated mice), which was markedly decreased by deleting BAP31 (LPS-exposed BAP31$^{-/-}$ mice versus LPS-only mice, Fig. 2H). Consequently, BAP31 deficiency decreased the total cell number, neutrophil count and protein concentration in the BALF.

3.3. Effects of BAP31 knockdown on PMN infiltration

Myeloperoxidase (MPO) functions as a symbol of neutrophils activation. Following the administration of LPS in mice, neutrophil accumulation in lung tissues was detected based on the neutrophil staining marker, MPO. As shown in Fig. 3A, the green signal for MPO staining in the LPS group was noticeably stronger than that of saline group, indicating that a large number of PMNs were recruited to the lung tissues of mice that received LPS treatment. However, the fluorescence signal in lung tissue of BAP31$^{-/-}$ mice was drastically weakened under the same LPS stimulation. A similar result was obtained by analyzing the numbers of neutrophils in randomly selected areas (Fig. 3B). To quantify neutrophil recruitment in lung, the MPO activity was evaluated (Fig. 3C). Compared with the saline group, MPO activity was significantly enhanced in lung tissues extracts collected from the LPS group. Nevertheless, MPO levels from lung extracts of LPS-administered BAP31$^{-/-}$ mice was drastically dropped (versus LPS- administered BAP31$^{+/+}$ mice). Both assays verified that the absence of BAP31 could

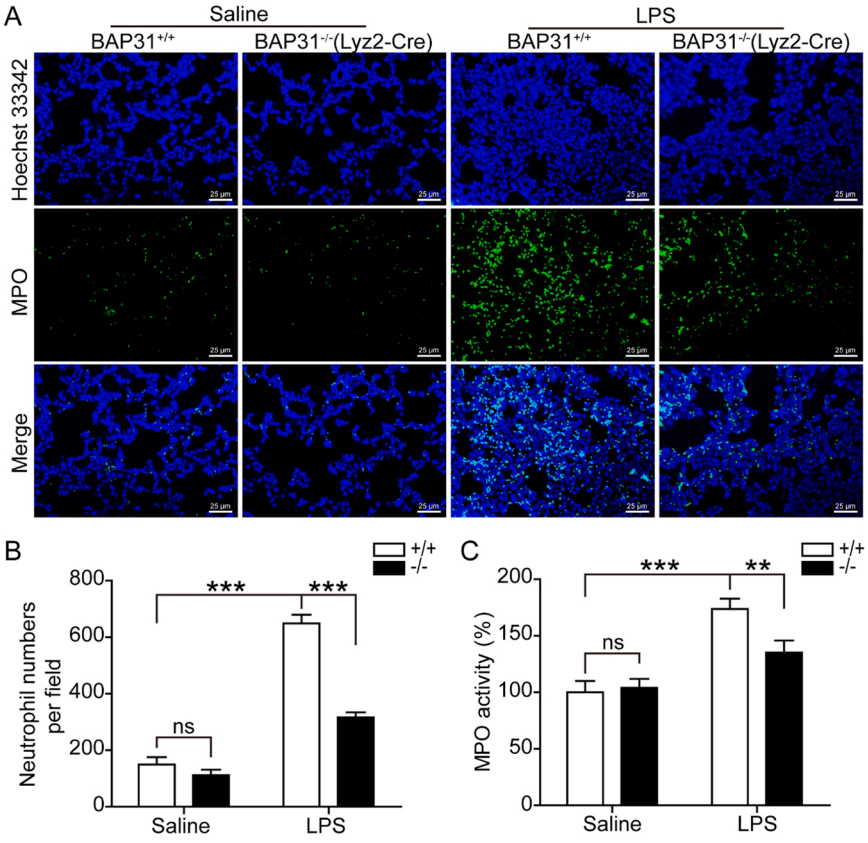

Fig. 3. Effects of BAP31 knockdown on neutrophil infiltration. (A) The observation of fluorescence distribution for neutrophil aggregation under a fluorescence microscope (Scale bars: 25 μm). (B) The number of neutrophils per section for lung tissue samples stained with MPO (Saline+BAP31$^{+/+}$, n = 3; Saline+BAP31$^{-/-}$, n = 3; LPS+BAP31$^{+/+}$, n = 3; LPS+BAP31$^{-/-}$, n = 3). (C) The detection of MPO activity (Saline+BAP31$^{+/+}$, n = 3; Saline+BAP31$^{-/-}$, n = 3; LPS+BAP31$^{+/+}$, n = 3; LPS+BAP31$^{-/-}$, n = 3). The values were shown as mean ± SEM, ** $p < 0.01$, *** $p < 0.001$. ns, not significant.

effectively block the influx of neutrophils into lung tissues.

3.4. Effects of BAP31 knockdown on adhesion of neutrophils

Neutrophil infiltration is a multi-step process that requires the participation of PMNs-ECs adhesion. For this reason, we continued to investigate leukocytes-endothelial interactions using intravital microscopy. In the resting mesenteric veins, leukocyte adhesion on the surface of vascular wall had no significant difference between BAP31$^{+/+}$ and BAP31$^{-/-}$ mice. Yet, LPS stimulation apparently strengthened the adhesive ability of leukocytes, which could be restrained by the lack of BAP31 (Fig. 4A). Meanwhile, the number of firmly adherent leukocytes in the LPS+BAP31$^{-/-}$ group was greatly descended (versus LPS+BAP31$^{+/+}$ group, Fig. 4B). These observations indicated that BAP31 depletion could enormously reduce the adhesive effects of PMNs on vascular wall.

To evaluate PMNs-ECs adhesion in *vitro*, we first isolated and purified neutrophils from the myeloid cell lineage of mice. Ly6G and CD11b typically act as special biomarkers on the surface of neutrophils (Li et al., 2010). The flow cytometry analysis was implemented to determine the purity of neutrophils stained with Ly6G and CD11b. Satisfactory results were obtained with high purity (91.1%, Fig. 4C, D). To investigate the relevance of BAP31 with neutrophil-endothelial cell adhesion, purified neutrophils were incubated with ECs (b.End3 cells) in *vitro*. As described in Fig. 4E, the LPS-stimulated group exerted an increased intensity of blue fluorescence, which was obviously decreased in the LPS+BAP31$^{-/-}$ group. In the case of LPS induction, the number of neutrophils adhering to ECs in BAP31$^{-/-}$ group exhibited a serious reduction by comparison with that of BAP31$^{+/+}$ group (Fig. 4F). These results revealed that BAP31 deficiency restrained the neutrophil-endothelial cell adhesion.

3.5. Effects of BAP31 knockdown on the expression of adhesion molecules in neutrophil

To further explore how BAP31 participates in the adhesion process, we scanned the mRNA levels of various adhesion molecules in neutrophils. As outlined in Fig. 5A, the mRNA expressions of CD11a, CD11c, CD29, CD49d and VLA-1 adhesion factors had no statistical significances with the loss of BAP31, whereas mRNA levels of PSGL-1, ESL-1, CD44, CD11b, L-selectin and CD18 were down-regulated at different degrees. After preliminary screening, the protein expression of three representative adhesion molecules (CD11b, CD18 and PSGL-1) was examined using Western blotting assay. There existed a noticeable reduction for the protein levels of CD11b, CD18 and PSGL-1 in BAP31$^{-/-}$ group (Fig. 5B). Meanwhile, the relative quantification of Western blot for these adhesion molecules showed a similar tendency (Fig. 5C-F). Thereafter, the surface expression of CD11b, CD18 and PSGL-1 on neutrophils was detected by flow cytometry (Fig. 5G-I). The analyses demonstrated that the expressions of CD11b, CD18 and PSGL-1 significantly declined with the absence of BAP31 at resting status. Following by LPS stimulation, the expression levels of these genes dramatically increased, which could be restrained by BAP31 knockdown. Similarly, the mean fluorescence intensity of CD11b, CD18 and PSGL-1 in LPS-challenged BAP31$^{-/-}$ group was apparently lower than that in LPS-only group (Fig. 5J-L). These data disclosed that BAP31 deficiency could inhibit the expression levels of related CAMs, thus decreasing the adhesiveness of PMNs to ECs.

It has been reported that BAP31 could bind with CD11b/CD18, thereby affecting its transport from secondary particles to the surface of cell membrane in human neutrophils (Zen et al., 2004). Based on this, we wondered the effects of BAP31 on the above adhesion molecules in mouse neutrophils. Immunoprecipitation assay was used to examine the combination of BAP31 with CD11b/CD18 and PSGL-1. After lysis of PMNs by NP40, the lysates were immunoprecipitated with IgG and

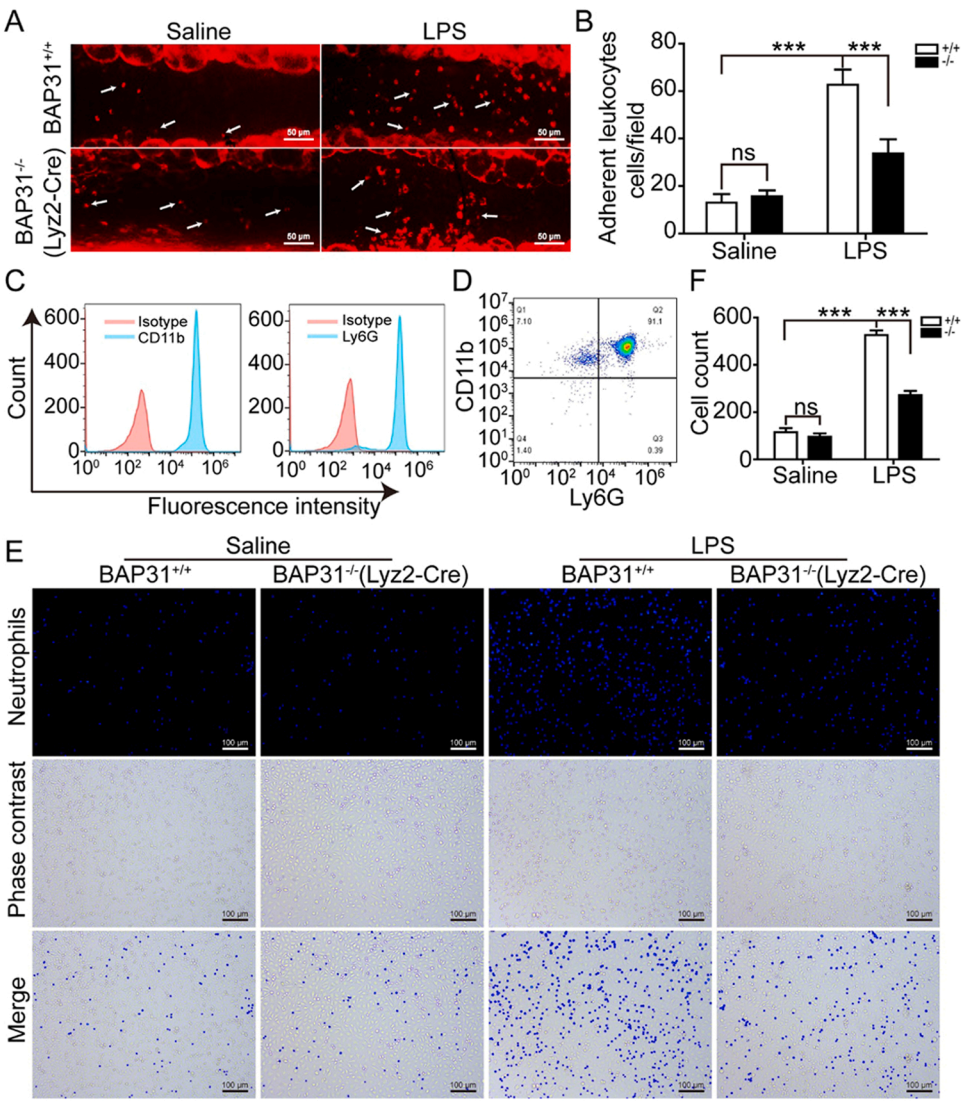

Fig. 4. Effects of BAP31 knockdown on in *vivo* and in *vitro* adhesion of neutrophils. (A) The representative intravital microscopy images using Rhodamine 6 G staining (Scale bars: 50 μm). (B) The quantitative analysis of firmly adhered leukocytes (Saline+BAP31$^{+/+}$, n = 3; Saline+BAP31$^{-/-}$, n = 3; LPS+BAP31$^{+/+}$, n = 3; LPS+BAP31$^{-/-}$, n = 3). (C, D) The pureness of neutrophil stained by surface markers CD11b and Ly6G was examined by flow cytometry. Neutrophils were defined as CD11b^{+} and Ly6G^{+}. (E) The In *vitro* PMNs-ECs adhesion was observed under fluorescence microscope (Scale bars: 100 μm). (F) Statistical analysis of adhered neutrophils (Saline+BAP31$^{+/+}$, n = 3; Saline+BAP31$^{-/-}$, n = 3; LPS+BAP31$^{+/+}$, n = 3; LPS+BAP31$^{-/-}$, n = 3). The values were shown as mean ± SEM, *** $p < 0.001$. ns, not significant.

BAP31 antibodies. Then, the immunoprecipitates were analyzed by Western blotting with anti-BAP31, anti-CD11b, anti-CD18 and anti-PSGL-1. As shown in Supplementary Fig. S4, BAP31 could directly combine with CD11b/CD18, but not PSGL-1. These results were tallied with those of a previous study, suggesting that BAP31 might be involved in the transport of CD11b/CD18 in mouse neutrophils.

3.6. *Effects of BAP31 knockdown on NF-κB signaling pathway*

Accumulating documents have illustrated that the expression of multitudinous adhesion molecules, such as CD11b, CD18 and PSGL-1, is inextricably linked with the NF-κB signaling pathway (Lee et al., 1996; Pfosser et al., 2010). In this connection, we investigated if BAP31 knockdown affected the NF-κB signaling pathway, thus restraining the expression of adhesion molecules. As shown in Fig. 6A and B, NF-κB p65 protein expression in the nucleus was checked by Western blotting. Under resting conditions, the level of NF-κB p65 in nucleus was suppressed in BAP31$^{-/-}$ group. After LPS intervention, the protein level of NF-κB p65 was substantially upregulated, which was restrained by the elimination of BAP31, indicating that BAP31 deficiency greatly reduced the translocation of NF-κB p65 from the cytoplasm to nucleus. Next, we analyzed the expression levels of p-IKKα/β, p-IκBα and IκBα in neutrophils (Fig. 6C-G). In quiescent states, BAP31 depletion visibly decreased the protein expressions of p-IKKα/β and p-IκBα, as well as increased IκBα expression. Upon LPS stimulation, a significant increase for p-IKKα/β, p-IκBα expressions and a decrease for IκBα expression were found, which could be reversed by BAP31 deletion. Notably, the elevated expression of IκBα implied that BAP31 elimination inhibited LPS-induced IκBα degradation. These data revealed that BAP31 knockdown could decrease the the expression of key adhesion molecules through inhibiting the NF-κB signaling pathway.

4. Discussion

Acute lung injury remains a frequent cause of morbidity and mortality in critically ill patient population. Clinically, the main manifestations of ALI are dyspnea and progressive hypoxemia (Proudfoot et al., 2011). BAP31, a carrier protein, participates in the transport process of multiple membrane proteins (Adachi et al., 1996; Annaert et al., 1997; Kim et al., 1994). For instance, a previous literature discovered that BAP31 can act as a regulator for the transport of CD11b/CD18 from secondary granules to the surface of the cell membrane in neutrophils (Zen et al., 2004). As an important CAM, the overexpression of CD11b/CD18 can promote PMNs infiltration, eventually leading to the occurrence of inflammation and tissue injury (Yuki et al., 2020). Encouraged by these findings, we speculated that BAP31 may play a pivotal role in ALI. To our knowledge, the function of BAP31 in ALI remains unclear owing to the lack of suitable animal models. Concerning

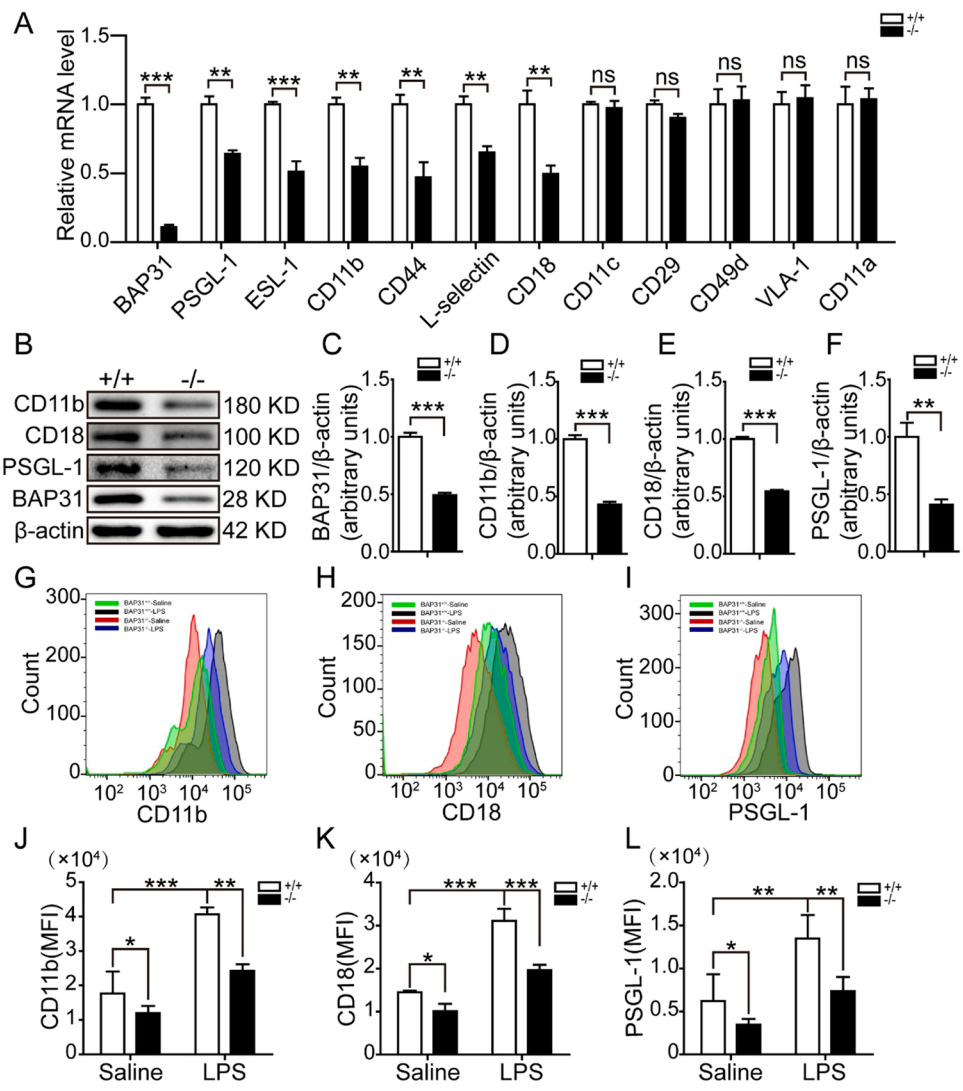

Fig. 5. Effects of BAP31 knockdown on the expression of adhesion molecules in neutrophils. (A) Real-time PCR analyses for diverse adhesion factors in neutrophils ($BAP31^{+/+}$, n = 3; $BAP31^{-/-}$, n = 3). (B) Protein expression of BAP31, CD11b, CD18 and PSGL-1 detected by Western blotting. (C-F) Quantitative analyses of Western blot for BAP31, CD11b, CD18 and PSGL-1 ($BAP31^{+/+}$, n = 3; $BAP31^{-/-}$, n = 3). (G-I) Flow cytometric detection for surface expression of CD11b, CD18 and PSGL-1 on neutrophils. (J-L) The analyses of mean fluorescence intensity for CD11b, CD18 and PSGL-1 (Saline+$BAP31^{+/+}$, n = 3; Saline+$BAP31^{-/-}$, n = 3; LPS+$BAP31^{+/+}$, n = 3; LPS+$BAP31^{-/-}$, n = 3). The values were shown as mean ± SEM, * $p < 0.05$, ** $p < 0.01$, *** $p < 0.001$. ns, not significant.

that the systemic knockdown of genes in mice can lead to an abnormality of biological functions, we introduced the Cre-loxP system to specifically eliminate target genes in a tissue/cell-type specific manner (Nagy, 2000; Sauer and Henderson, 1988). To elucidate the role of BAP31 in LPS-induced ALI, we initially created myeloid-specific BAP31 knockdown mice via the Lyz2-Cre/loxP system. In this study, the genotype of mice was determined by PCR analysis of the DNA genome. The results of RT-qPCR and Western blotting demonstrated that mRNA and protein levels of BAP31 expression exerted a significant decrease in $BAP31^{-/-}$ mice compared with $BAP31^{+/+}$ mice. Fortunately, the body weight, the number of leukocytes and PMNs in both groups of mice showed no statistical differences, indicating that the physiological and growth status of mice were almost unaffected by the absence of BAP31. Consistently, myeloid-specific BAP31 knockdown did also not affect normal growth and development of lung.

Subsequently, the injection of LPS into mice by tail vein was used to establish the ALI model. Stimulation LPS into $BAP31^{+/+}$ mice for 24 h could cause typical alterations of histopathology and morphology in lungs, which suggested the success of model establishment. Compared with LPS-treated $BAP31^{+/+}$ mice, the pathological abnormalities of lungs in LPS-treated $BAP31^{-/-}$ mice were obviously improved. Additionally, BAP31 deficiency had a protective effect on the reduction of body weight induced by LPS stimulation. Based on the degree of neutrophil infiltration, alveolar congestion, wall thickening and hemorrhage, lung injury was scored to quantify the differences. It was found that a decreased score occurred in LPS+$BAP31^{-/-}$ mice. A growing number of studies have reported that LPS challenge can cause an elevation for lung water content, massive influx of proteins and inflammatory cells into the alveolar space (Bhattacharya and Matthay, 2013). Usually, lung W/D ratio is used as an index to measure the severity of pulmonary edema (Yang et al., 2019). Our results declared that the lung W/D ratio, protein concentration, total leukocyte counts and neutrophil numbers were apparently lessened in LPS-stimulated $BAP31^{-/-}$ mice, further indicating an obvious remission of lung edema and neutrophil infiltration. Therefore, elimination of BAP31 contributed to attenuating the extent of pulmonary impairments.

During the early phase of ALI, rapid and appropriate recruitment of leukocytes from the circulation to inflammatory site is essential for defense against the invasion of microbial pathogens and pathological impairments (Havixbeck et al., 2016). However, exuberant infiltration and aggregation of leukocytes will exacerbate ALI via secreting some proinflammatory mediators (Imai et al., 2008). Additionally, an increasing body of clinical and experimental studies have found that neutrophil accumulation into inflammation location is often accompanied by the release of MPO (Zhang et al., 2019). The fluctuation of MPO level in plasma can reflect the function and activity status of neutrophils. Accordingly, MPO activity often serves as a sensitive and specific hallmark of neutrophil activation (de Souza Ferreira et al., 2012). To

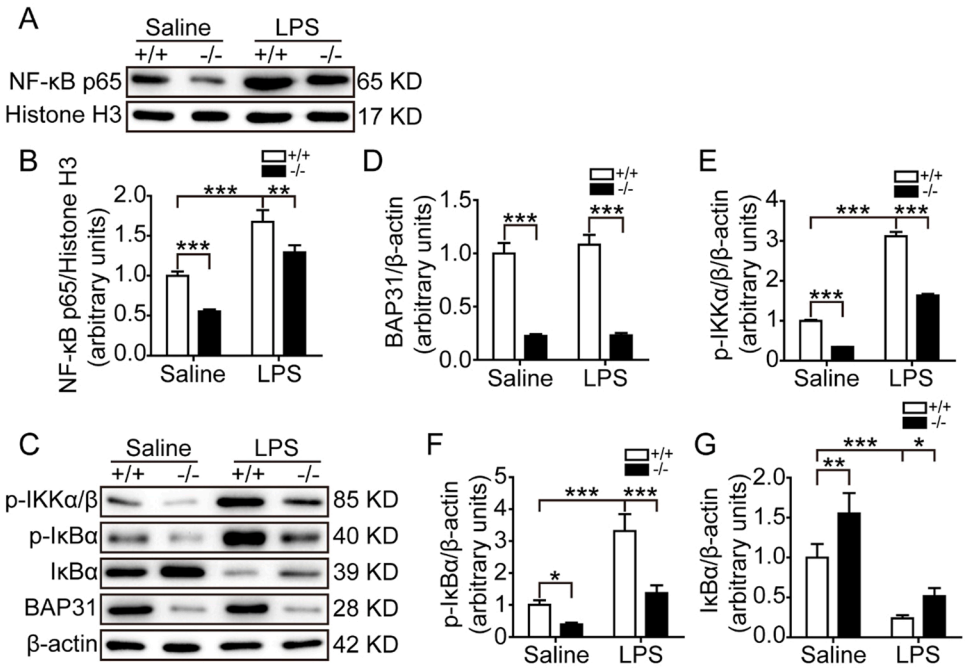

Fig. 6. Effects of BAP31 knockdown on NF-κB signaling pathway. (A) Protein expression of NF-κB p65 in nucleus detected by Western blotting. (B) Quantification analyses of Western blot for NF-κB p65 (Saline+BAP31$^{+/+}$, n = 3; Saline+BAP31$^{-/-}$, n = 3; LPS+BAP31$^{+/+}$, n = 3; LPS+BAP31$^{-/-}$, n = 3). (C) The expression levels of phospho-IKKα/β, phosphor-IκBα and IκBα checked by Western blotting. (D-G) Quantitative analyses of Western blot for p-IKKα/β, p-IκBα and IκBα (Saline+BAP31$^{+/+}$, n = 3; Saline+BAP31$^{-/-}$, n = 3; LPS+BAP31$^{+/+}$, n = 3; LPS+BAP31$^{-/-}$, n = 3). The values were shown as mean ± SEM, * $p < 0.05$, ** $p < 0.01$, *** $p < 0.001$. ns, not significant.

evaluate the influence of BAP31 on neutrophil infiltration, fluorescence microscopy and colorimetry were conducted to qualitatively and quantitatively monitor MPO variations. Our results demonstrated that MPO levels were highly induced after LPS excitation, which was restrained by the loss of BAP31. The decreased MPO level indicated a reduction for neutrophils infiltrating into the pulmonary alveoli and interstitium, which was consistent with previously histological observations. Intimate PMNs-ECs adhesion has been widely assumed as a demanded stage for neutrophil infiltration. Herein, adhesive assays were carried out in *vitro* and in *vivo* to further investigate if BAP31 impacted neutrophils-ECs adhesion. Intravital microscopy showed that the adhesion of PMNs to vessel wall was significantly descended with BAP31 deficiency. Simultaneously, a similar effect was observed in the co-culture pattern of neutrophils and ECs. Based on these results, we conjectured that the decreased adhesion of neutrophils caused by BAP31 knockdown might be due to the influence of BAP31 on the expression or function of related adhesion molecules.

Several investigations have suggested that neutrophil rolling and adhesion are subjected to the regulation of different adhesion molecules (Ley et al., 2007). The selectin family (P-, E- and L-selectins) can recognize and bind to their glycoprotein counter-ligands, thus dominantly mediating leukocyte rolling (Kansas, 1996). Nevertheless, secondary adhesion of PMNs is largely dependent on the regulation of integrin family and CD44 molecule expressed on neutrophils (Konrad et al., 2019). For this purpose, RT-PCR analysis was performed to inspect mRNA levels of an array of adhesive factors. Upon the loss of BAP31 in PMNs, mRNA levels of CD49d, CD29, CD11c, CD11a and VLA-1 were almost unaffected, while the mRNA levels of PSGL-1, CD11b, CD18, L-selectin, ESL-1 and CD44 were declined at varying degrees. Remarkably, CD11b/CD18 is an important member of integrin family and has been directly implicated in cellular adhesion (Yuki and Hou, 2020). PSGL-1, a well-studied selectin ligand, structurally and functionally modulates neutrophil rolling and signal transduction (Zarbock et al., 2009). Subsequently, the protein levels of CD11b, CD18 and PSGL-1 were measured by Western blotting. By comparison with BAP31$^{+/+}$ group, their expression was down-regulated in BAP31$^{-/-}$ group. Meanwhile, the flow analysis results displayed a decreased surface expression of CD11b, CD18 and PSGL-1 on neutrophils from BAP31$^{-/-}$ mice. To further examine how BAP31 influence CD11b/CD18 and PSGL-1, an immunoprecipitation experiment was performed. Our analysis revealed that BAP31 bound directly to CD11b/CD18 in mouse neutrophils, which was consistent with previous findings in human neutrophils (Zen et al., 2004). Considering the co-localization of BAP31 and CD11b/CD18, we conjectured that BAP31 was possibly a regulator of intracellular transport and expression of CD11b/CD18 in mice neutrophils. In addition, BAP31 failed to integrate with PSGL-1, suggesting that BAP31 only regulated PSGL-1 expression. On the basis of these findings, we hypothesized that BAP31 could reduce neutrophil-endothelial cell adhesion via modulating the expression of CD11b, CD18 and PSGL-1, thus ameliorating ALI.

A series of literatures have reported that NF-κB activation is intimately associated with the expression of multiple adhesion molecules (e.g. CD11b, CD18 and PSGL-1) (Dorrington and Fraser, 2019). Normally, NF-κB is sequestered in the cytoplasm by forming a complex with IκB protein. Upon LPS stimulation, IκB kinase (IKK) is rapidly activated, which leads to the phosphorylation and degradation of IκB. Immediately, NF-κB dissociates from the complex and enters into nucleus, where it binds to gene promoter regions and initiates the transcription of adhesion molecules (Zhong et al., 2018). We aimed to determine whether BAP31 deficiency impacts the NF-κB signaling pathway, thereby inhibiting the expression of adhesion molecules. In LPS+BAP31$^{-/-}$ group, we observed an apparent downregulation for NF-κB level in the nucleus, indicating that nuclear translocation of NF-κB was prominently decreased with the loss of BAP31. Moreover, a significant decline for p-IKKα/β, p-IκBα and an elevation for IκBα expression were noticed in LPS+BAP31$^{-/-}$ group, manifesting that IKK/NF-κB signaling pathway was dominantly abrogated by the elimination of BAP31. Therefore, the effect of BAP31 on CAMs expression might be governed by NF-κB.

This study remained some limitations. Previous literatures have showed that BAP31 can bind to CD11b/CD18 and impact their trafficking to the cell membrane surface. In addition, our researches proved that BAP31 could directly combine with CD11b/CD18 and influence CD11b/CD18 expressions in mouse neutrophils. Considering that BAP31 had dual effects on the transcription and transport of adhesion molecule CD11b/CD18, we wondered whether the dual role of BAP31 is regulated by some signaling pathways and the degradation of related proteins in these pathways. For this reason, the unsettled doubts deserve further

study as a future research direction. Despite these limitations, preliminary results revealed the mitigation effect of BAP31 deficiency on LPS-induced ALI to some extent.

5. Conclusions

In summary, our results confirmed that BAP31 deficiency reduced neutrophil infiltration by lowering neutrophil-endothelial adhesivity, thereby effectively alleviating LPS-triggered ALI. The underlying mechanism may be attributed to the fact that BAP31 knockdown down-regulated the expression of CD11b, CD18 and PSGL-1 possibly by inhibiting the NF-κB signaling pathway. These findings indicated BAP31 as a potential protein for regulating the pathogenesis of ALI/ARDS.

Funding

This research was supported by the Liaoning Revitalization Talents Program (XLYC1902063), Key Research and Development Plan of Liaoning Province (2020JH2/10300080), National Natural Science Foundation of China (31670770, 2016YFC1302402, 31370784), and the Fundamental Research Funds for the Central Universities of China (N2120004).

CRediT authorship contribution statement

Guo-xun Li: Conceptualization, Methodology, Validation, Investigation, Writing – original draft. **Xiao-han Jiang:** Validation, Investigation, Data curation. **Jing-nan Zang:** Validation, Investigation, Data curation. **Ben-zhi Zhu**: Validation, Investigation, Data curation. **Cong-cong Jia:** Formal analysis. **Kun-wei Niu:** Formal analysis. **Xia Liu**: Formal analysis. **Rui Jiang**: Resources, Visualization, Project administration. **Bing Wang**: Conceptualization, Resources, Visualization, Supervision, Project administration, Funding acquisition. All authors have read and agreed to the published version of the manuscript.

Conflict of interest

The authors declare that they have no conflict of interest.

Appendix A. Supplementary material

Supplementary data associated with this article can be found in the online version at doi:10.1016/j.biocel.2022.106299.

References

Adachi, T., Schamel, W.W., Kim, K.M., Watanabe, T., Becker, B., Nielsen, P.J., Reth, M., 1996. The specificity of association of the IgD molecule with the accessory proteins BAP31/BAP29 lies in the IgD transmembrane sequence. EMBO J. 15 (7), 1534–1541.

Annaert, W.G., Becker, B., Kistner, U., Reth, M., Jahn, R., 1997. Export of cellubrevin from the endoplasmic reticulum is controlled by BAP31. J. Cell Biol. 139 (6), 1397–1410. https://doi.org/10.1083/jcb.139.6.1397.

Bartee, E., Eyster, C.A., Viswanathan, K., Mansouri, M., Donaldson, J.G., Früh, K., 2010. Membrane-associated RING-CH proteins associate with Bap31 and target CD81 and CD44 to lysosomes. PLoS One 5 (12), e15132. https://doi.org/10.1371/journal.pone.0015132.

Berger, M., O'Shea, J., Cross, A.S., Folks, T.M., Chused, T.M., Brown, E.J., Frank, M.M., 1984. Human neutrophils increase expression of C3bi as well as C3b receptors upon activation. J. Clin. Investig. 74 (5), 1566–1571. https://doi.org/10.1172/JCI111572.

Bhattacharya, J., Matthay, M.A., 2013. Regulation and repair of the alveolar-capillary barrier in acute lung injury. Annu. Rev. Physiol. 75 (1), 593–615. https://doi.org/10.1146/annurev-physiol-030212-183756.

Butt, Y., Kurdowska, A., Allen, T.C., 2016. Acute lung injury: a clinical and molecular review. Arch. Pathol. Lab. Med 140 (4), 345–350. https://doi.org/10.5858/arpa.2015-0519-RA.

Cacciagli, P., Sutera-Sardo, J., Borges-Correia, A., Roux, J.C., Dorboz, I., Desvignes, J.P., Badens, C., Delepine, M., Lathrop, M., Cau, P., Lévy, N., Girard, N., Sarda, P., Boespflug-Tanguy, O., Villard, L., 2013. Mutations in BCAP31 cause a severe X-linked phenotype with deafness, dystonia, and central hypomyelination and disorganize the Golgi apparatus. Am. J. Hum. Genet. 93 (3), 579–586. https://doi.org/10.1016/j.ajhg.2013.07.023.

Chen, J., Guo, H., Jiang, H., Namusamba, M., Wang, C., Lan, T., Wang, T., Wang, B., 2019. A BAP31 intrabody induces gastric cancer cell death by inhibiting p27kip1 proteasome degradation. Int. J. Cancer 144 (8), 2051–2062. https://doi.org/10.1002/ijc.31930.

Crockett-Torabi, E., 1998. Selectins and mechanisms of signal transduction. J. Leukoc. Biol. 63 (1), 1–14.

Dianzani, C., Collino, M., Lombardi, G., Garbarino, G., Fantozzi, R., 2003. Substance P increases neutrophil adhesion to human umbilical vein endothelial cells. Br. J. Pharmacol. 139 (6), 1103–1110. https://doi.org/10.1038/sj.bjp.0705344.

Dorrington, M.G., Fraser, I.D.C., 2019. NF-κB signaling in macrophages: dynamics, crosstalk, and signal integration. Front. Immunol. 10 (4), 705. https://doi.org/10.3389/fimmu.2019.00705.

Farley, F.W., Soriano, P., Steffen, L.S., Dymecki, S.M., 2000. Widespread recombinase expression using FLPeR (flipper) mice. Genesis 28 (3–4), 106–110.

Fine, N., Barzilay, O., Sun, C., Wellappuli, N., Tanwir, F., Chadwick, J.W., Oveisi, M., Tasevski, N., Prescott, D., Gargan, M., Philpott, D.J., Dror, Y., Glogauer, M., 2019. Primed PMNs in healthy mouse and human circulation are first responders during acute inflammation. Blood Adv. 3 (10), 1622–1637. https://doi.org/10.1182/bloodadvances.2018030585.

Friedrichs, K., Adam, M., Remane, L., Mollenhauer, M., Rudolph, V., Rudolph, T.K., Andrié, R.P., Stöckigt, F., Schrickel, J.W., Ravekes, T., Deuschl, F., Nickenig, G., Willems, S., Baldus, S., Klinke, A., 2014. Induction of atrial fibrillation by neutrophils critically depends on CD11b/CD18 integrins. PLoS One 9 (2), e89307. https://doi.org/10.1371/journal.pone.0089307.

Havixbeck, J.J., Rieger, A.M., Wong, M.E., Hodgkinson, J.W., Barreda, D.R., 2016. Neutrophil contributions to the induction and regulation of the acute inflammatory response in teleost fish. J. Leukoc. Biol. 99 (2), 241–252. https://doi.org/10.1189/jlb.3HI0215-064R.

Hidari, K.I., Weyrich, A.S., Zimmerman, G.A., McEver, R.P., 1997. Engagement of P-selectin glycoprotein ligand-1 enhances tyrosine phosphorylation and activates mitogen-activated protein kinases in human neutrophils. J. Biol. Chem. 272 (45), 28750–28756. https://doi.org/10.1074/jbc.272.45.28750.

Hou, S., Ding, H., Lv, Q., Yin, X., Song, J., Landén, N.X., Fan, H., 2014. Therapeutic effect of intravenous infusion of perfluorocarbon emulsion on LPS-induced acute lung injury in rats. PLoS One 9 (1), e87826. https://doi.org/10.1371/journal.pone.0087826.

Imai, Y., Kuba, K., Neely, G.G., Yaghubian-Malhami, R., Perkmann, T., van Loo, G., Ermolaeva, M., Veldhuizen, R., Leung, Y.H., Wang, H., Liu, H., Sun, Y., Pasparakis, M., Kopf, M., Mech, C., Bavari, S., Peiris, J.S., Slutsky, A.S., Akira, S., Hultqvist, M., Holmdahl, R., Nicholls, J., Jiang, C., Binder, C.J., Penninger, J.M., 2008. Identification of oxidative stress and Toll-like receptor 4 signaling as a key pathway of acute lung injury. Cell 133 (2), 235–249. https://doi.org/10.1016/j.cell.2008.02.043.

Issekutz, A.C., Rowter, D., Springer, T.A., 1999. Role of ICAM-1 and ICAM-2 and alternate CD11/CD18 ligands in neutrophil transendothelial migration. J. Leukoc. Biol 117–126. https://doi.org/10.1002/jlb.65.1.117.

Iwasawa, R., Mahul-Mellier, A.L., Datler, C., Pazarentzos, E., Grimm, S., 2011. Fis1 and Bap31 bridge the mitochondria-ER interface to establish a platform for apoptosis induction. EMBO J. 30 (3), 556–568. https://doi.org/10.1038/emboj.2010.346.

Jerke, U., Rolle, S., Purfürst, B., Luft, F.C., Nauseef, W.M., Kettritz, R., 2013. β2 integrin-mediated cell-cell contact transfers active myeloperoxidase from neutrophils to endothelial cells. J. Biol. Chem. 288 (18), 12910–12919. https://doi.org/10.1074/jbc.M112.434613.

Jia, C.C., Du, J., Liu, X., Jiang, R., Huang, Y., Wang, T., Hou, Y., Wang, B., 2018. B-cell receptor-associated protein 31 regulates the expression of valosin-containing protein through Elf2. Cell Physiol. Biochem. 51 (4), 1799–1814. https://doi.org/10.1159/000495682.

Johnson-Léger, C., Imhof, B.A., 2003. Forging the endothelium during inflammation: pushing at a half-open door. Cell Tissue Res. 314 (1), 93–105. https://doi.org/10.1007/s00441-003-0775-4.

Kansas, G.S., 1996. Selectins and their ligands: current concepts and controversies. Blood 88 (9), 3259–3287.

Kim, K.M., Adachi, T., Nielsen, P.J., Terashima, M., Lamers, M.C., Köhler, G., Reth, M., 1994. Two new proteins preferentially associated with membrane immunoglobulin D. EMBO J. 13 (16), 3793–3800. https://doi.org/10.1002/j.1460-2075.1994.tb06690.x.

Konrad, F.M., Wohlert, J., Gamper-Tsigaras, J., Ngamsri, K.C., Reutershan, J., 2019. How adhesion molecule patterns change while neutrophils traffic through the lung during inflammation. Mediat. Inflamm. 2019, 1–16. https://doi.org/10.1155/2019/1208086.

Ladasky, J.J., Boyle, S., Seth, M., Li, H., Pentcheva, T., Abe, F., Steinberg, S.J., Edidin, M., 2006. Bap31 enhances the endoplasmic reticulum export and quality control of human class I MHC molecules. J. Immunol. 177 (9), 6172–6181. https://doi.org/10.4049/jimmunol.177.9.6172.

Lee, D.H., Tam, S.S., Wang, E., Taylor, G.R., Plante, R.K., Lau, C.Y., 1996. The NF-kappa B inhibitor, tepoxalin, suppresses surface expression of the cell adhesion molecules CD62E, CD11b/CD18 and CD106. Immunol. Lett. 53 (2–3), 109–113. https://doi.org/10.1016/s0165-2478(96)02619-3.

Ley, K., Laudanna, C., Cybulsky, M.I., Nourshargh, S., 2007. Getting to the site of inflammation: the leukocyte adhesion cascade updated. Nat. Rev. Immunol. 7 (9), 678–689. https://doi.org/10.1038/nri2156.

Li, P., Li, M., Lindberg, M.R., Kennett, M.J., Xiong, N., Wang, Y., 2010. PAD4 is essential for antibacterial innate immunity mediated by neutrophil extracellular traps. J. Exp. Med. 207 (9), 1853–1862. https://doi.org/10.1084/jem.20100239.

Maas, S.L., Soehnlein, O., Viola, J.R., 2018. Organ-specific mechanisms of transendothelial neutrophil migration in the lung, liver, kidney, and aorta. Front. Immunol. 9, 2739. https://doi.org/10.3389/fimmu.2018.02739.

Muller, W.A., 2013. Getting leukocytes to the site of inflammation. Vet. Pathol. 50 (1), 7–22. https://doi.org/10.1177/0300985812469883.

Mutlu, G.M., Machado-Aranda, D., Norton, J.E., Bellmeyer, A., Urich, D., Zhou, R., Dean, D.A., 2007. Electroporation-mediated gene transfer of the Na^+, K^+-ATPase rescues endotoxin-induced lung injury. Am. J. Respir. Crit. Care Med. 176 (6), 582–590. https://doi.org/10.1164/rccm.200608-1246OC.

Nagy, A., 2000. Cre recombinase: the universal reagent for genome tailoring. Genesis 26 (2), 99–109.

Ng, F.W., Nguyen, M., Kwan, T., Branton, P.E., Nicholson, D.W., Cromlish, J.A., Shore, G. C., 1997. p28 Bap31, a Bcl-2/Bcl-XL- and procaspase-8-associated protein in the endoplasmic reticulum. J. Cell Biol. 139 (2), 327–338. https://doi.org/10.1083/jcb.139.2.327.

Niu, K., Xu, J., Cao, Y., Hou, Y., Shan, M., Wang, Y., Xu, Y., Sun, M., Wang, B., 2017. BAP31 is involved in T cell activation through TCR signal pathways. Sci. Rep. 7 (1), 44809. https://doi.org/10.1038/srep44809.

Pfosser, A., El-Aouni, C., Pfisterer, I., Dietz, M., Globisch, F., Stachel, G., Trenkwalder, T., Pinkenburg, O., Horstkotte, J., Hinkel, R., Sperandio, M., Hatzopoulos, A.K., Boekstegers, P., Bals, R., Kupatt, C., 2010. NF-kappaB activation in embryonic endothelial progenitor cells enhances neovascularization via PSGL-1 mediated recruitment: novel role for LL37. Stem Cells 28 (2), 376–385. https://doi.org/10.1002/stem.280.

Proudfoot, A.G., McAuley, D.F., Griffiths, M.J., Hind, M., 2011. Human models of acute lung injury. Dis. Models Mech. 4 (2), 145–153. https://doi.org/10.1242/dmm.006213.

Sauer, B., Henderson, N., 1988. Site-specific DNA recombination in mammalian cells by the Cre recombinase of bacteriophage P1. Proc. Natl. Acad. Sci. USA 85 (14), 5166–5170. https://doi.org/10.1073/pnas.85.14.5166.

Silvestre-Roig, C., Braster, Q., Ortega-Gomez, A., Soehnlein, O., 2020. Neutrophils as regulators of cardiovascular inflammation. Nat. Rev. Cardiol. 17 (6), 327–340. https://doi.org/10.1038/s41569-019-0326-7.

de Souza Ferreira, C., Araújo, T.H., Ângelo, M.L., Pennacchi, P.C., Okada, S.S., de Araújo Paula, F.B., Migliorini, S., Rodrigues, M.R., 2012. Neutrophil dysfunction induced by hyperglycemia: modulation of myeloperoxidase activity. Cell Biochem. Funct. 30 (7), 604–610. https://doi.org/10.1002/cbf.2840.

Standiford, T.J., Ward, P.A., 2016. Therapeutic targeting of acute lung injury and acute respiratory distress syndrome. Transl. Res. 167 (1), 183–191. https://doi.org/10.1016/j.trsl.2015.04.015.

Tan, S.M., 2012. The leucocyte β2 (CD18) integrins: the structure, functional regulation and signalling properties. Biosci. Rep. 32 (3), 241–269. https://doi.org/10.1042/BSR20110101.

Wang, B., Pelletier, J., Massaad, M.J., Herscovics, A., Shore, G.C., 2004. The yeast split-ubiquitin membrane protein two-hybrid screen identifies BAP31 as a regulator of the turnover of endoplasmic reticulum-associated protein tyrosine phosphatase-like B. Mol. Cell. Biol. 24 (7), 2767–2778. https://doi.org/10.1128/MCB.24.7.2767-2778.2004.

Wang, B., Heath-Engel, H., Zhang, D., Nguyen, N., Thomas, D.Y., Hanrahan, J.W., Shore, G.C., 2008. BAP31 interacts with Sec61 translocons and promotes retrotranslocation of CFTRDeltaF508 via the derlin-1 complex. Cell 133 (6), 1080–1092. https://doi.org/10.1016/j.cell.2008.04.042.

Wang, B., Nguyen, M., Chang, N.C., Shore, G.C., 2011. Fis1, Bap31 and the kiss of death between mitochondria and endoplasmic reticulum. EMBO J. 30 (3), 451–452. https://doi.org/10.1038/emboj.2010.352.

Wang, Q., Doerschuk, C.M., 2002. The signaling pathways induced by neutrophil-endothelial cell adhesion. Antioxid. Redox Signal. 4 (1), 39–47. https://doi.org/10.1089/152308602753625843.

Ware, L.B., 2006. Pathophysiology of acute lung injury and the acute respiratory distress syndrome. Semin. Respir. Crit. Care Med. 27 (4), 337–349. https://doi.org/10.1055/s-2006-948288.

Wee, J.L., Schulze, K.E., Jones, E.L., Yeung, L., Cheng, Q., Pereira, C.F., Costin, A., Ramm, G., van Spriel, A.B., Hickey, M.J., Wright, M.D., 2015. Tetraspanin CD37 regulates β2 integrin-mediated adhesion and migration in neutrophils. J. Immunol. 195 (12), 5770–5779. https://doi.org/10.4049/jimmunol.1402414.

Xu, J.L., Li, L.Y., Wang, Y.Q., Li, Y.Q., Shan, M., Sun, S.Z., Yu, Y., Wang, B., 2018. Hepatocyte-specific deletion of BAP31 promotes SREBP1C activation, promotes hepatic lipid accumulation, and worsens IR in mice. J. Lipid Res. 59 (1), 35–47. https://doi.org/10.1194/jlr.M077016.

Yang, J., Hirata, T., Croce, K., Merrill-Skoloff, G., Tchernychev, B., Williams, E., Flaumenhaft, R., Furie, B.C., Furie, B., 1999. Targeted gene disruption demonstrates that P-selectin glycoprotein ligand 1 (PSGL-1) is required for P-selectin-mediated but not E-selectin-mediated neutrophil rolling and migration. J. Exp. Med. 190 (12), 1769–1782. https://doi.org/10.1084/jem.190.12.1769.

Yang, Z., Ji, W., Li, M., Qi, Z., Huang, R., Qu, J., Wang, H., Wang, H., 2019. Protective effect of nimesulide on acute lung injury in mice with severe acute pancreatitis. Am. J. Transl. Res. 11 (9), 6024–6031.

Yuki, K., Hou, L., 2020. Role of β2 integrins in neutrophils and sepsis. e00031-20 Infect. Immun. 88 (6). https://doi.org/10.1128/IAI.00031-20.

Zarbock, A., Müller, H., Kuwano, Y., Ley, K., 2009. PSGL-1-dependent myeloid leukocyte activation. J. Leukoc. Biol. 86 (5), 1119–1124. https://doi.org/10.1189/jlb.0209117.

Zen, K., Utech, M., Liu, Y., Soto, I., Nusrat, A., Parkos, C.A., 2004. Association of BAP31 with CD11b/CD18. Potential role in intracellular trafficking of CD11b/CD18 in neutrophils. J. Biol. Chem. 279 (43), 44924–44930. https://doi.org/10.1074/jbc.M402115200.

Zhang, J., Zhao, J., Jiang, W.J., Shan, X.W., Yang, X.M., Gao, J.G., 2012. Conditional gene manipulation: cre-ating a new biological era. J. Zhejiang Univ. Sci. B 13 (7), 511–524. https://doi.org/10.1631/jzus.B1200042.

Zhang, X., Zheng, J., Yan, Y., Ruan, Z., Su, Y., Wang, J., Huang, H., Zhang, Y., Wang, W., Gao, J., Chi, Y., Lu, X., Liu, Z., 2019. Angiotensin-converting enzyme 2 regulates autophagy in acute lung injury through AMPK/mTOR signaling. Arch. Biochem. Biophys. 672, 108061 https://doi.org/10.1016/j.abb.2019.07.026.

Zhong, L., Simard, M.J., Huot, J., 2018. Endothelial microRNAs regulating the NF-κB pathway and cell adhesion molecules during inflammation. FASEB J. 32 (8), 4070–4084. https://doi.org/10.1096/fj.201701536R.